

Report No. ORNL/TM-6806, 1979 (unpublished).

³R. A. Dandl *et al.*, Oak Ridge National Laboratory

Report No. ORNL/TM-6457, 1978 (to be published).

⁴E. F. Jaeger *et al.*, Phys. Rev. Lett. **40**, 866 (1978).

⁵R. D. Hazeltine *et al.*, Science Applications, Inc.,

Report No. SAI-02379-664LJ, 1979 (to be published).

⁶L. M. Kovrizhnykh, Zh. Eksp. Teor. Fiz. **56**, 877 (1969) [Sov. Phys. JETP **29**, 475 (1969)].

⁷R. A. Dandl *et al.*, Oak Ridge National Laboratory Report No. ORNL/TM-4941, 1975 (unpublished).

Spontaneous, Three-Dimensional, Constant-Energy Implosion of Magnetic Mirror Fields

Paul M. Bellan

California Institute of Technology, Pasadena, California 91125

(Received 8 June 1979)

Experimental and theoretical results are presented concerning a method for providing three-dimensional spontaneous implosion of a magnetic mirror field. This is achieved by making the mirror field a propagating macroscopic wave in a medium for which the wave velocity is a slowly changing function of position. Slowing down of the magnetic mirror wave causes WKB steepening and shortening—i.e., three-dimensional field compression—in a manner wherein the total magnetic field energy stays constant.

Rapidly increasing the current in the field coils of a magnetic mirror is effective for both heating mirror-confined particles and increasing their density.¹ However, this compression technique is inefficient, because magnetic energy, W_B , scales as B^2 , while particle energy, T_{\perp} , scales only as B . Hence, more energy goes into creating new magnetic field lines than into heating particles. The imploding liner² partially avoids this problem by decreasing (in a flux-conserving manner) the field cross-sectional area as B increases so that W_B will scale as B . Unfortunately this method involves difficult engineering problems if a repetitive system is wanted, as for a fusion reactor.

I present here experimental and theoretical results on an entirely new method of adiabatic compression which does not involve liners and which provides a three-dimensional compression at essentially *constant* magnetic field energy. This is achieved by compressing the magnetic field volume in all three dimensions so that as B increases, $W_B = B^2 V / 2\mu_0$ stays constant. The three-dimensional nature of this compression gives both three-dimensional heating and a greater density increase than two-dimensional compression. Because only passive components are used and because the compression ratio is determined solely by the system geometry (and not by the energy input), the effective result is a spontaneously imploding, magnetic mirror.

In this scheme a moving magnetic mirror is created by arranging for the mirror field to be a propagating disturbance in some medium. It becomes, in effect, a macroscopic wave, carrying

particles trapped in its trough. WKB theory states that the characteristic axial length and intensity of such a propagating disturbance can change if the characteristic wave velocity of the medium is a slowly varying function of position in the medium. In particular, in regions where the wave velocity decreases, the magnetic-mirror wave shortens and steepens in a manner wherein its total energy stays constant. When this wave steepening occurs, adiabatic compression of particles trapped by the mirror will result. The particles are heated in the perpendicular direction ($T_{\perp} \propto B$), in the parallel direction ($T_{\parallel} \propto \lambda^{-2}$, where λ is the axial extent of the mirror field), and are compressed in three dimensions ($n \propto B/\lambda$). The compression occurs at constant (except for diamagnetic effects) W_B , and the compression ratio depends only on the geometric properties of the medium, and not on the energy input.

A practical realization of the above field compressor has been constructed. In this device (c.f. Fig. 1) coils comprising a long solenoid are connected to capacitors, each having capacitance C , so as to form a variation on a lumped-element delay line.³ Pulses injected onto the delay line propagate along it with a characteristic velocity determined by the inductances, capacitances, and inter-coil spacings. In particular, a double-humped⁴ pulse of the type shown in Fig. 1(a) also propagates down the delay line at the characteristic velocity. Associated with this current pulse is an axially propagating double-humped solenoidal magnetic field—i.e., the axially propagating magnetic mirror. This solenoid delay line is thus the

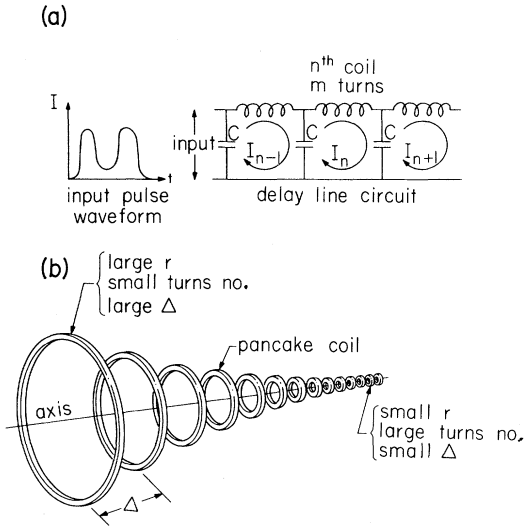


FIG. 1. (a) Circuit and input pulse; (b) physical configuration. Δ is the intercoil spacing. For the device described here coils 1-7 have $r=4$ cm, $m=10$, $\Delta=3$ cm; coils 8-15 are the tapered section; coils 16-24 have $r=2$ cm, $m=19$, $\Delta=2$ cm.

desired medium on which a macroscopic magnetic-mirror wave propagates. The delay-line properties are gradually changed with respect to axial position in a manner whereby the wave velocity slows down; from WKB theory this steepens the magnetic-mirror wave, i.e., increases its intensity and decreases its axial extent.

Figure 1(b) shows a qualitative sketch of the 24-coil, 50-cm-long solenoid delay line field compressor. The first seven coils have coil radius $r=4$ cm, turns number $m=10$ turns, and intercoil spacing $\Delta=3$ cm; these are followed by an eight-coil tapered section which connects to the last nine coils for which $r=2$ cm, $m=19$ turns, $\Delta=2$ cm. The wire diameter is 1.6 mm, and the small-diameter end is terminated in a 10- Ω resistor to prevent reflections. A double pulse is injected into the large-diameter end and the axially translating magnetic mirror field is observed using a 100-turn magnetic pickup loop connected to a passive RC integrator circuit. The field profile at a particular time after the pulse injection is measured by translating the pickup probe along the solenoid axis and recording the field intensity as a function of axial position. By repeating this for a sequence of times, the moving magnetic mirror is observed. Figure 2 shows the results of two such measurements. Note how the low-intensity magnetic mirror at earlier times is compressed into a short, high-intensity mirror field

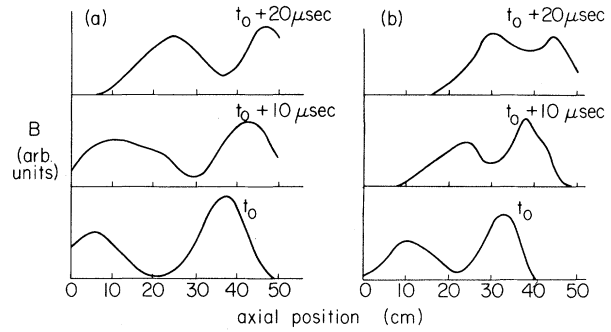


FIG. 2. Observed propagating compressing mirrors, input pulse: (a) 20 μ sec max, 20 μ sec min, 20 μ sec max (equal amplitude maxima); (b) 5 μ sec max, 17 μ sec min, 9 μ sec max (first maximum has 40% more amplitude than second).

at later times.

An approximate scaling analysis has been made, based on (i) long pulses ($\lambda \gg r, \Delta$ where λ is the characteristic axial extent of the mirror field), and (ii) closely spaced coils (each coil links considerable flux from adjacent coils). From (i) coils within a distance λ of the n th coil have nearly the same current as I_n , the current in the n th coil, and the field is solenoidal in nature so that

$$B \approx \mu_0 m I_n / \Delta, \quad (1)$$

where μ_0 is the permeability of free space. From (ii) and Eq. (1), the n th coil links the flux

$$\Phi_n \approx \mu_0 m^2 I_n \pi r^2 / \Delta. \quad (2)$$

Summing the voltages [cf. Fig. 1(a)] around the n th mesh of the delay line gives a wave equation for I_n ,

$$\frac{\mu_0 m^2}{\Delta} \pi r^2 \frac{d^2 I_n}{dt^2} - \frac{1}{C} \frac{d^2 I_n}{dn^2} = 0 \quad (3)$$

or equivalently for $I(z)$,

$$\frac{\mu_0 m^2}{\Delta} \pi r^2 \frac{d^2 I(z)}{dz^2} - \frac{\Delta^2}{C} \frac{d^2 I(z)}{dz^2} = 0. \quad (4)$$

(Here Taylor expansions of $I_{n \pm 1}$ and the relation $dz = \Delta dn$ have been used.)

For slowly varying r, Δ , and m , WKB theory and Eq. (3) show that $I_n \propto \Delta^{1/4} / m^{1/2} r^{1/2}$, which with Eq. (1) gives

$$B \propto m^{1/2} / \Delta^{3/4} r^{1/2}, \quad (5)$$

while from Eq. (4) and WKB theory

$$\lambda \propto \Delta^{3/2} / m r. \quad (6)$$

Thus W_B , which scales as $B^2 r^2 \lambda$, stays constant.

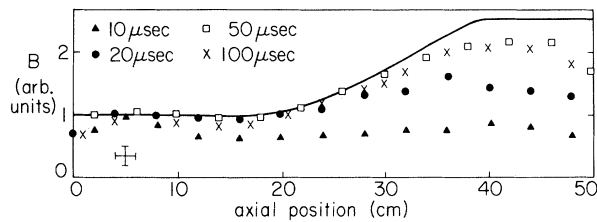


FIG. 3. Observed B dependence on position compared with Eq. (5) (solid line) for four different pulse durations. Bars at lower left show typical error.

Hence, to achieve an increasing field intensity having decreasing volume, all that is required is to gradually increase the quantity $m^{1/2}/\Delta^{3/4}r^{1/2}$ for successive coils in the delay line (this was done in the tapered section of the delay line described here). The discreteness (finite Δ) of the delay line and the finiteness of λ/r causes pulse broadening which competes with the WKB steepening. This broadening can be used to increase the field minima of the mirror and hence the compression ratio, but if allowed to go too far it completely erases the mirror central dip. For Fig. 2(a) a relatively long input pulse was used and the peak B approximately follows the WKB scaling; for Fig. 2(b) shorter pulses were used and mirror compression comes primarily from pulse broadening filling in the central minimum. Figure 3 shows a quantitative comparison between Eq. (5) and single input pulses having different durations; as expected longer pulses follow Eq. (5) better.

An important advantage of the solenoid–delay-line constant-energy compressor (CEC) is that the system can spend proportionally more time in the final, compressed state than in the initial state, a direct consequence of the wave–slowing-down nature of the compression. Hence, time spent at low temperatures where collisions may be important can be minimized, and time spent in the final compressed state where collisions are small can be maximized. This is exactly what one typically would want for a fusion device.

Various combinations of m , Δ , and r scalings are possible—the most obvious are (a) constant flux ($B \propto r^{-2}$, $\lambda \propto r^2$, $\Delta \propto m^{2/3}r^2$, density $\propto r^{-4}$), (b) constant geometry ($B \propto r^{-3/2}$, $\lambda \propto r$, $\Delta \propto m^{2/3}r^{4/3}$, density $\propto r^{-3}$), and (c) constant T_{\perp}/T_{\parallel} ratio ($B \propto r^{-4/3}$, $\lambda \propto r^{2/3}$, $\Delta \propto m^{2/3}r^{10/9}$, density $\propto r^{-8/3}$). The compression time scales, for a given coil configuration, as \sqrt{C} ; faster compressions require operation at higher voltages.

An obvious application of the CEC is the ion-

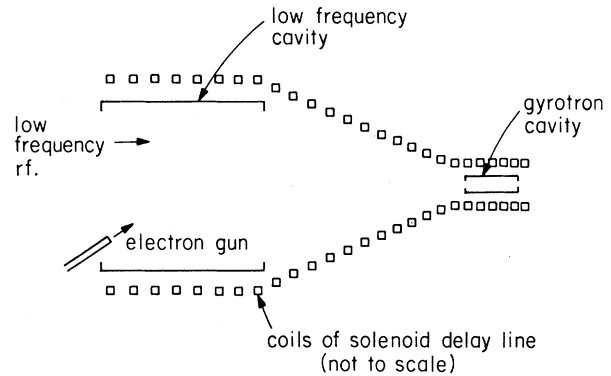


FIG. 4. Proposed pulsed gyrotron.

ring compression fusion reactor⁵—the axial contraction involved in the CEC compression is especially appropriate for generating field-reversed particle rings. The original idea,⁵ which envisioned moving a “relatively small magnetic mirror (10–20% of the local field strength)” into a high-field region, required a static magnetic field on which was imposed a small moving perturbation, created by firing a sequence of capacitor banks (as in David, Rej, and Fleischmann⁶). With the CEC, the complicated switching network and the energy stored both in the static magnetic field and the unfired capacitor banks are all eliminated. Device scalings⁷ which preserve the field profile (i.e., constant Q) show that $C \sim l^3$ and characteristic time $T \sim l^2$, where l is the device linear dimension. Scaling the device described here up to the dimensions of Ref. 5 (l increases 250 \times) gives $C \approx 3$ F, $T \sim 1$ sec; for $B = 14$ kG typical operating voltages would be $\sim 10^4$ V.

Figure 4 illustrates how the CEC could also be used for a new pulsed gyrotron.⁸ Here, an energetic electron ring is created by cyclotron-resonance heating in a large low-frequency microwave cavity; using the CEC the electrons are then compressed and translated to a smaller cavity where, by means of the gyrotron mechanism, they emit intense microwaves at a much higher frequency. Because the peak magnetic field and peak energy density can be much higher than in conventional gyrotrons, extremely high frequencies and pulsed powers should be obtainable this way.

The experimental and theoretical results presented here are preliminary in nature; better data will be available shortly when a larger-scale (~ 2 kJ, 10^3 density compression) compressor—now being designed—is put into operation and tested for actual particle heating. Quantitative

theories of pulse broadening, and finite- β effects are now being developed.

This work was supported in part by the Alfred P. Sloan Foundation.

¹A. W. Trivelpiece, R. E. Pechacek, and C. A. Kapetanakis, *Phys. Rev. Lett.* **21**, 1436 (1968).

²P. J. Turchi and W. L. Baker, *J. Appl. Phys.* **44**, 4936 (1973).

³J. Millman and H. Taub, *Pulse and Digital Circuits* (McGraw-Hill, New York, 1956), p. 291.

⁴Delay lines have been previously used to produce

single-humped (i.e., no mirror trapping) traveling magnetic fields for accelerating plasmas [J. Marshall, in *Proceedings of the Second United Nations Conference of Peaceful Uses of Atomic Energy*, United Nations, Geneva, 1958 (unpublished), Vol. 31, p. 341; L. M. Lidsky and D. J. Rose, *Rev. Sci. Instrum.* **34**, 1223 (1963)].

⁵H. H. Fleischmann and T. Kammash, *Nucl. Fusion* **15**, 1143 (1975).

⁶H. A. Davis, D. J. Rej, and H. H. Fleischmann, *Phys. Rev. Lett.* **39**, 744 (1977).

⁷P. Bellan, to be published.

⁸J. L. Hirshfield and V. L. Granatstein, *IEEE Trans. Microwave Theory Tech.* **25**, 522 (1977).

Nonlinear Stabilization of the Ion-Beam-Cyclotron Instability

J. R. Myra and C. S. Liu

Department of Physics and Astronomy, University of Maryland, College Park, Maryland 20742

(Received 24 May 1979)

The nonlinear evolution of a single, coherent, electrostatic, ion-cyclotron wave driven unstable by a cold-ion beam directed along the magnetic field is studied. When the beam energy density is large compared to the thermal energy density of the background plasma, saturation occurs by the nonlinear ion gyrofrequency shift of the background ions. Saturation amplitudes are estimated and nonlinear oscillations and solitons are shown to occur.

Ion-cyclotron waves driven unstable by the free energy of particle beams or currents are common in many laboratory and space plasmas. Satellite measurements in the auroral zone of the earth's magnetosphere show a definite correlation between upstreaming energetic ions and coherent electrostatic fluctuations at the proton cyclotron frequency.¹ In laboratory plasmas, especially mirror machines and tokamaks, beam heating is of great importance, thus beam-plasma interactions may play an important role. Experimentally, ion-cyclotron waves are commonly observed.² The prediction of saturation levels for the beam-driven cyclotron instabilities, and a clearer understanding of the nonlinear physics involved is thus of considerable interest.

In the present paper, we follow the early-time, nonlinear evolution of a single coherent Bernstein wave driven unstable by a cold ion beam di-

rected along the magnetic field, $\vec{B} = -B\hat{e}_z$. The wave, at frequency ω and wavenumber $\vec{k} = (k_x, 0, k_z)$, is supported by a Maxwellian plasma of ion density N_i and temperature T on which is superimposed an ion beam of density N_b , particle mass m_b , and velocity u . The Maxwellian electrons have density $N_e = N_i + N_b$. We assume that $(\omega - n\Omega)/k_z v_i \gg 1$, $(N_b/N_i)k_x^2 \bar{\rho}_i^2 < 1$, $k^2 \lambda_{Di}^2 \ll 1$ where $v_i^2 = T_i/m_i$, $\lambda_{Di}^2 = T_i/4\pi N_i e^2$, $\bar{\rho}_i^2 = v_i^2/\Omega_i^2$. For $\omega \sim n\Omega = neB/m_i c$, the linear responses of the various species are

$$n_i = -(N_i e \varphi / T) [1 - \omega \Lambda_n / (\omega - n\Omega)],$$

$$n_b = N_b e k_x^2 \varphi / m_b (\omega - k_z u)^2, \quad n_e = N_e e \omega \delta / T,$$

where $\delta = 1$ for the Boltzmann electrons ($\omega/k_z v_e < 1$) and $\delta = 0$ for fluid electrons ($\omega/k_z v_e > 1$). In the above, $\Lambda_n = I_n(b) e^{-b}$ with $b = k_x^2 \bar{\rho}_i^2 = k_x^2 T/m_i \Omega_i^2$. Setting $n_i + n_b = n_e$, the linear dispersion relation is

$$(\omega - \omega_0)(\omega - \omega_0 - \Delta)^2 = \epsilon [1 + (\omega - \omega_0)/(\omega_0 - n\Omega)], \quad (1)$$

where

$$\epsilon = (N_b/N_i)(m_i/m_b) [k_x^2 v_i^2 / (1 + \delta - \Lambda_n)] (\omega_0 - n\Omega),$$

$$\omega_0 = (1 + \delta)n\Omega / (1 + \delta - \Lambda_n), \quad \text{and } \Delta = k_z u - \omega_0 \text{ and } N_e \approx N_i$$

has been used. In the absence of the beam ω_0 is the usual Bernstein frequency and Δ is the mismatch between the beam mode and the Bernstein mode. Maximum growth occurs for $\Delta \approx 0$, in which case we